

To appear in the *International Journal of Computer Mathematics*
Vol. xx, No. xx, xx 2014, 1–9

Original Research

Sensitivity Analysis and Variance Reduction in a Stochastic NDT Problem

R. H. De Staelen^{a*} and K. Beddek^b

^a*Numerical Analysis and Mathematical Modeling, Ghent University, Gent 9000, Belgium;*

^b*THEMIS dept., Électricité de France R&D, Clamart 92141, France*

(submitted August 27, 2013; accepted January 28, 2014)

In this paper, we present a framework to deal with uncertainty quantification in case where the ranges of variability of the random parameters are ill-known. Namely the physical properties of the corrosion product (magnetite) which frequently clogs the tube support plate of steam generator, which is inaccessible in nuclear power plants. The methodology is based on Polynomial Chaos (PC) for the direct approach and on Bayesian inference for the inverse approach. The direct Non-Intrusive Spectral Projection (NISP) method is first employed by considering prior probability densities and therefore constructing a PC surrogate model of the large-scale NDT finite element model. To face the prohibitive computational cost underlying the high dimensional random space, an adaptive sparse grid technique is applied on NISP resulting in drastic time reduction. The PC surrogate model, with reduced dimensionality, is used as a forward model in the Bayesian procedure. The posterior probability densities are then identified by inferring from few noisy experimental data. We demonstrate effectiveness of the approach by identifying the most influential parameter in the clogging detection as well as a variability range reduction.

Keywords: uncertainty quantification; polynomial chaos; bayesian inference; non destructive testing

AMS Subject Classification: 62F15; 35R30; 62P30; 35Q61 (MSC2010)

1. Introduction

Quantifying the impact of uncertainties of input data on solutions of forward and inverse electromagnetic numerical models has received large interest during the last decade, e.g. in the biomedical EEG problem [4, 5], in population biology and biofilm growth [3, 10] and in particular in eddy current inspection. The latter is a technique used for, among others, the detection of cracks in tubes and magnetite clogging of the Tube Support Plate (TSP) in steam generators at nuclear power plants [2, 11]. The detection of clogging is investigated with a Non Destructive Testing (NDT) eddy current procedure with an axial bobbin probe. The Finite Element model used to reproduce the technique assumes that material properties of magnetite and of the TSP are known exactly. However, to this date, it is not possible to get a pure sample of the clogged magnetite. Moreover, the material properties of the TSP may change due to aging. Experimental measurements show an important variability on permeability and conductivity of the magnetite. This paper deals with the determination of the probability density distribution of the

*Corresponding author. Email: rob.destaelen@ugent.be

permeability and conductivity of the magnetite and the TSP. We show how a surrogate model computed by employing a Polynomial Chaos (PC) expansion can be used to infer a posterior probability density distribution of the random input parameters from experimental measurement using the Bayesian inference method.

Furthermore, we are interested in the identification of the most influential random variables. The PC expansion is used to propagate prior uncertainty distributions through the finite element forward model; it yields a polynomial expression of the forward solution over the support of the prior distribution. By the use of Sobol indices we are able to quantify the contribution of each parameter to the total variance of the solution.

To construct a probability distribution of the model parameters we start with uniform priors and use Bayesian inference to obtain posterior densities based on probe measurements. This results in a variance reduction and updated information about the model parameters.

2. Numerical model

Let \mathcal{D} be a spatial domain divided into M_1 conducting disjoint subdomains and M_2 non-conducting disjoint subdomains. The permeability $\mu(\mathbf{x}, \theta)$ and conductivity $\sigma(\mathbf{x}, \theta)$ of \mathcal{D} are assumed to be random fields, where \mathbf{x} denotes the spatial variable and θ the outcome belonging to the random event space Θ . The magnetic field \mathbf{H} , the induction field \mathbf{B} and the electric field \mathbf{E} generated in \mathcal{D} by a deterministic source term \mathbf{J}_s are then random fields defined on $\mathcal{D} \times \Theta$. They verify the harmonic Maxwell's equations in quasi-static regime, where we denote ω the frequency and j the imaginary unit. We assume that some boundary conditions on \mathbf{B} and \mathbf{E} are given on the domain \mathcal{D} , see [7]. The differential operators, curl and divergence, operate only on the spatial dimension \mathbf{x} . As $\mathbf{B}(\mathbf{x}, \theta)$ is divergence free, it derives from a magnetic vector stochastic potential $\mathbf{A}(\mathbf{x}, \theta)$ such that $\mathbf{B}(\mathbf{x}, \theta) = \nabla \times \mathbf{A}(\mathbf{x}, \theta)$. Also, Faraday's law implies that $\mathbf{E}(\mathbf{x}, \theta) = -j\omega\mathbf{A}(\mathbf{x}, \theta) - \nabla\varphi(\mathbf{x}, \theta)$, where $\varphi(\mathbf{x}, \theta)$ is the electric scalar stochastic potential.

Using the stochastic magnetic constitutive relation $\mathbf{B}(\mathbf{x}, \theta) = \mu(\mathbf{x}, \theta)\mathbf{H}(\mathbf{x}, \theta)$ and substituting yields the stochastic magneto-harmonic problem

$$\nabla \times \left(\frac{\nabla \times \mathbf{A}(\mathbf{x}, \theta)}{\mu(\mathbf{x}, \theta)} \right) + \sigma(\mathbf{x}, \theta) \left(j\omega\mathbf{A}(\mathbf{x}, \theta) + \nabla\varphi(\mathbf{x}, \theta) \right) = \mathbf{J}_s(\mathbf{x}). \quad (1)$$

To numerically solve the problem, the spatial and stochastic spaces are approximated by finite dimensional spaces. Whitney finite elements are used to discretize the spatial dimension. In the considered NDT model, the spatial dimension is discretized by 1,419,948 Whitney elements leading to 1,789,946 spatial unknowns. The stochastic dimension is approximated by a Legendre PC. The latter method will be described in the section 3.1. The skin effect due to the presence of eddy current in the TSP is taken into account by considering the Surface Impedance Boundary Condition (SIBC) method. It is a special 2D finite element method which avoids the meshing of the whole TSP. The considered clogging of a quatrefoil TSP configuration is the so-called "case 5" in [11] and corresponds to a full blockage of a foil with 5mm magnetite deposit, see Fig. 1.

The deterministic simulation procedure consists in computing the Sax ratio. Such an indicator measures, because of magnetite presence, the alteration of the imaginary part of the differential flux between the two probes. For further details on the deterministic simulation procedure, we refer to [11].

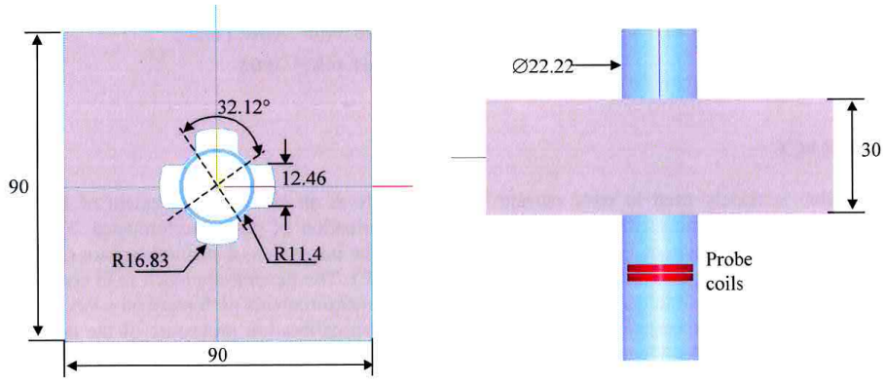


Figure 1. Geometry of the problem (in mm).

3. Uncertainty quantification and Bayesian inference

Because of the nature of the deposit and the aging of the TSP, deterministic simulations turn out to be imprecise. Therefore, stochastic studies are engaged at Électricité de France (EdF) in order to quantify the influence of the variability in material properties on the measured probe flux. Two kinds of direct approaches may be used to take into account uncertainties of the input data: sampling or statistical techniques (Monte Carlo Simulation, Latin Hypercube Sampling, etc.) and probabilistic methods. The sampling methods are simple, but unfortunately have a low rate of convergence. The second are Polynomial Chaos (PC) methods, where the randomness is expressed in the Wiener-Askey PC expansion [13, 14] and non-intrusive methods are used to derive the probability density function of the stochastic dependence. As the probability density and range of variation of magnetite's relative permeability and conductivity are unknown, we will use the most uninformative density, i.e. making them uniform distributed variables. We consider the relative permeability (in henry per meter) and conductivity (in siemens per meter) of the magnetite and the TSP as independent. Relative permeability of the magnetite is taken uniform on the interval [1.3, 2.7] and its conductivity uniform on the interval [45, 75]. For the TSP, the relative permeability is considered uniform on [60, 100] and the conductivity uniform on [17E5, 18E5]. By introducing measurements (more information) we will refine the densities of the considered parameters accordingly.

3.1 Polynomial chaos expansion

The PC expansion was first introduced by Wiener [13] to represent stochastic processes. It was applied in mechanics by Ghanem and Spanos [6] to solve stochastic differential equations on a probability space (Ω, \mathcal{F}, P) where \mathcal{F} is the σ -algebra of the event space Ω and P is the probability measure. The solution of a stochastic model, having as input parameters the vector $\boldsymbol{\xi}(\theta) = (\xi_1(\theta), \dots, \xi_n(\theta))$ of n independent random variables, can be written as mapping $\Phi : \Omega^m \rightarrow \mathbb{R}$. Thus the model output Φ is a random variable and one writes $\Phi(\theta) = \Phi(\boldsymbol{\xi}(\theta)) = \Phi(\xi_1(\theta), \dots, \xi_m(\theta))$. The PC expansion refers to the representation of the random variable $\Phi(\theta)$ belonging to the Hilbert space $\mathcal{L}^2(\Omega, \mathcal{F}, P)$ as a linear combination of multivariate polynomials $\Psi_i(\boldsymbol{\xi}(\theta))$, [14]:

$$\Phi(\theta) = \sum_{\alpha \in \mathbb{N}^m} \Phi_{\alpha} \Psi_{\alpha}(\boldsymbol{\xi}(\theta)) \quad (2)$$

where α is a m -uplet containing the order of the univariate polynomials used to construct the multivariate polynomial. The polynomials $\{\Psi_i\}$ are orthogonal with respect to the joint probability measure $f_{\xi} = \prod_{1 \leq i \leq m} f_{\xi_i}$. That is to say

$$E[\Psi_i(\theta)\Psi_j(\theta)] = \int_{\Omega} \Psi_i(\theta)\Psi_j(\theta) dP(\theta) = \int_{\mathbb{R}^m} \Psi_i(\xi)\Psi_j(\xi)f_{\xi} d\xi = \delta_{ij} \quad (3)$$

where $E[\cdot]$ denotes expectation and δ_{ij} the Kronecker symbol. To accomplish this polynomial representation, Wiener used Hermite polynomials in terms of Gaussian random variables (homogeneous chaos) to represent Gaussian processes. In order to deal with more diverse stochastic fields, the Wiener homogeneous chaos is generalized to the Wiener-Askey polynomial chaos (gPC), [14]. The multivariate polynomials of the gPC are constructed by tensoring univariate polynomials ψ_i which are orthogonal with respect to the probability measure of ξ_i . The Askey scheme [14] gives the correspondence between these univariate polynomials and the probability measure. In practice (2) is truncated to polynomials of order up to p . If we denote S_p^d the space of the m -uplets α which satisfy $|\alpha| = \sum_i \alpha_i \leq p$, the total number of polynomials in the gPC is equal to $\binom{m+p}{p} - 1$.

3.2 Adaptive Non-Intrusive Spectral Projection

The non-intrusive PC method aims to obtain a functional representation of a numerical model response by expanding the random dimension in the Wiener-Askey PC. In other words, we seek a representation of the form (2). The deterministic coefficients Φ_{α} are computed by calling the deterministic numerical model with a set of input data. The Non-Intrusive Spectral Projection (NISIP) method consists of projecting the stochastic solution onto the orthogonal gPC polynomial basis $\{\Psi_{\alpha}\}$. The deterministic projection coefficients Φ_{α} are then given by $\Phi_{\alpha} = E[\Phi\Psi_{\alpha}]/E[\Psi_{\alpha}^2]$. The multi-dimensional integrals $E[\Phi\Psi_{\alpha}]$ are evaluated with a set of deterministic simulations obtained by sampling methods (Monte Carlo Simulation, Latin Hypercube Sampling), full tensor-product quadrature (Gauss, Clenshaw-Curtis) or Smolyak sparse grids.

Gaussian quadrature rules are known to be the most effective rules, they are exact for polynomials of order $2n - 1$ when using n points of quadrature. However, these rules can not be used in an adaptive integration procedure because the grid points of the Gaussian rules are not nested (grid points of level q do not include grid points of level $q - 1$). As mentioned in [1], the nested Gauss-Patterson rules are well suitable in an adaptive procedure. These schemes do not provide higher convergence than Gaussian quadrature rules but are more competitive than Clenshaw-Curtis rules. For a given level $0 \leq l \leq 7$, the Gauss-Patterson scheme has $2^{l+1} - 1$ quadrature points and can integrate polynomials of order $3 \cdot 2^l - 1$ exactly.

Using a sparse grid with nested one-dimensional quadrature rules in an adaptive procedure leads finally to an isotropic sparse grid in the sense that the different dimensions of integration are discretized in the same and equal manner. Even though such a procedure can reduce the deterministic simulation number, the size of the sparse grid may still be high when the number of random variables is important. Moreover, integrating in the same way along each stochastic dimension may turn out to be not adapted when the numerical model is sensitive for only one or a small number of stochastic dimensions.

The anisotropic adaptive procedure is a way to reduce the number of quadrature points by taking advantage of this difference in sensitivity along the stochastic dimensions. In this work, an adaptive algorithm based on non-isotropic nested Gauss-Patterson formulas [1] is used to take into account the model global sensitivity to the input random variables.

This procedure results in the computation of the mean of the random flux.

Then the smoothness of the random flux is estimated from the sparse grid that was obtained in the anisotropic adaptive NISP. A polynomial interpolation of the random flux is constructed by taking advantage of the order of exactness of the obtained sparse grid. Further details and performances of such method are described in [1].

3.3 Global sensitivity analysis

The PC-based Sobol indices are obtained from the so called Sobol or ANOVA decomposition [12]. The Sobol decomposition of Y reads

$$Y(\boldsymbol{\xi}) = y_0 + \sum_{1 \leq i \leq n} Y_i(\xi_i) + \sum_{1 \leq i < j \leq n} Y_{ij}(\xi_i, \xi_j) + \cdots + Y_{1\dots n}(\boldsymbol{\xi}), \quad (4)$$

and is unique. The terms of the decomposition are orthogonal “term by term” and their integrals for each argument are zero. Due to the independence of the random variables, one can show that the variance D of $Y(\boldsymbol{\xi})$ can be written as

$$D = \sum_{1 \leq i \leq n} D_i + \sum_{1 \leq i < j \leq n} D_{ij} + \cdots + D_{1\dots n} \quad (5)$$

where $D_{i\dots j}$ are called partial or conditional variances. They express the contribution of the random variables ξ_i, \dots, ξ_j to the total variability of the model. Due to the orthogonality of the decomposition (4), the total variance D is the sum of the partial variances of Y . The Sobol indices are defined by $S_{i\dots j} = D_{i\dots j}/D$. If the model $Y(\boldsymbol{\xi})$ is expressed in the form (2) then (4) becomes

$$Y(\boldsymbol{\xi}) = y_0 + \sum_{1 \leq i \leq n} \sum_{\boldsymbol{\alpha} \in S_p^1} y_{\boldsymbol{\alpha}} \Psi_{\boldsymbol{\alpha}}(\xi_i) + \sum_{1 \leq i < j \leq n} \sum_{\boldsymbol{\alpha} \in S_p^{1,2}} y_{\boldsymbol{\alpha}} \Psi_{\boldsymbol{\alpha}}(\xi_i, \xi_j) + \cdots + \sum_{\boldsymbol{\alpha} \in S_p^{1\dots n}} y_{\boldsymbol{\alpha}} \Psi_{\boldsymbol{\alpha}}(\boldsymbol{\xi}), \quad (6)$$

and the first order Sobol indices are $S_{i\dots j} = \frac{1}{D} \sum_{\boldsymbol{\alpha}^* \in S_p^n} y_{\boldsymbol{\alpha}^*}^2$, where $\boldsymbol{\alpha}^*$ verifies $\sum_{k=1}^n \alpha_k^* - \sum_{k=i}^j \alpha_k^* = 0$.

3.4 Bayesian Inference (inverse method)

For inverse problems *Bayesian inference (BI)* offers a rigorous foundation for inference from uncertain forward models and noisy data. It is a natural procedure for incorporating prior information, and a quantitative assessment of uncertainty in the results. Contrary to other methods, the output of Bayesian inference is not solely a value, but a probability distribution that captures all available information about the parameters. From this distribution, one may compute marginal distributions, estimate moments or make other predictions. We first introduce Bayes' theory and well known results.

Suppose θ is a parameter of interest, τ a real function and T an estimator of $\tau(\theta)$. A *loss function* is any real-valued function $L(t; \theta)$ such that it is non negative for all t and zero when $t = \tau(\theta)$. The *risk function* R_T associated to a loss function L is its expectation $R_T(\theta) = \mathbb{E}[L(T; \theta)]$. If one has prior knowledge about the parameter location, one might want to use an estimator that has a small risk for values of θ that are most likely to occur in a given experiment. This is modeled by treating θ as a random variable

whose distribution f_θ captures the prior knowledge. The *Bayesian risk* of an estimator T relative to a risk function R_T and prior f_θ is $A_T = \mathbb{E}[R_T(\theta)] = \int_{-\infty}^{+\infty} R_T(t) f_\theta(t) dt$. If an estimator has the smallest Bayesian risk, then it is referred to as a *Bayesian estimator*.

As can be found in [9], the Bayesian estimator T of $\tau(\theta)$ under the squared error loss function $L(T; \theta) = [T - \tau(\theta)]^2$ is given by the mean of τ with respect to the posterior density based on the sample observations $\mathbf{x} = (x_1, \dots, x_n)$ from X ;

$$f_{\theta|X}(t|\mathbf{x}) = \frac{1}{\nu(t)} f_{X|\theta}(\mathbf{x}|t) f_\theta(t), \quad f_{X|\theta}(\mathbf{x}|t) = \prod_{i=1}^n f_{X|\theta}(x_i|t)$$

with $f_{X|\theta}$ the probability distribution function of X given θ , called the likelihood and $\nu(t)$ a normalizing factor.

We emphasize the fact that a Bayesian estimator depends on the choice of loss function. Under the squared error loss function it corresponds to the mean of the posterior distribution, it is sometimes called the *minimum mean square error (MMSE)* estimator [8]. This is the estimator we will use in what follows.

The inverse model consists of retrieving the input parameters, the properties of TSP and magnetite, given a probe flux measurement. The stochastic flux prediction Y is in fact undergoing some error – probe noise and model error, so $Y = \hat{Y} + \epsilon$, where ϵ is a random variable with density ϕ_ϵ . A typical assumption is ϵ being a zero mean normal variable, so $\epsilon \sim N(0, \sigma_\epsilon^2)$. In this case the likelihood becomes

$$\phi_{Y|\xi}(y|\xi) = \phi_\epsilon(y - \hat{Y}(\xi)).$$

We have a posterior probability density $\phi_{\xi|Y}$ for the model parameters (up to a normalizing factor) defined by the product of the likelihood $\phi_{Y|\xi}$ with the prior density ϕ_ξ . The latter embodies all prior knowledge on these parameters. In our case the prior is uninformative so equal to a constant. Under the squared error loss function, the Bayesian estimator of the input parameters is found as the mean of the posterior density. To fix

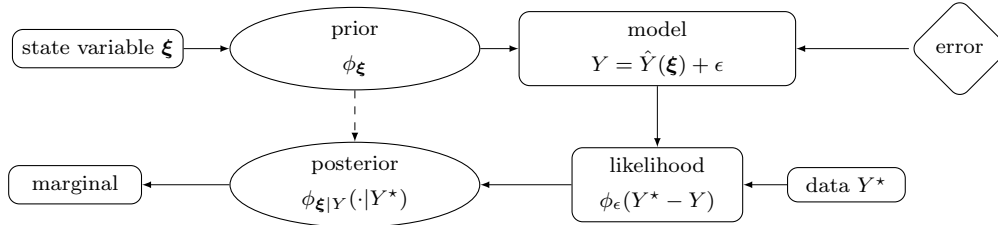


Figure 2. Different components in the Bayesian procedure with error calibration.

the model inference error σ_ϵ , we use a sample of 25 SAX ratios. Since, based on the Sobol indices (see next section), the permeability of the magnetite is the most influential parameter, we fix the other parameters to their mean and pick the σ_ϵ which enables us to retrieve the prior (uniform distribution) of μ_r^m . A general procedure of the Bayesian inference is reported in Fig. 2 together with the calibration of the error.

4. Results and discussion

We consider 4 independent random variables: the relative permeability of magnetite is uniform on the interval [1.3, 2.7], the conductivity of magnetite on the interval [45, 75],

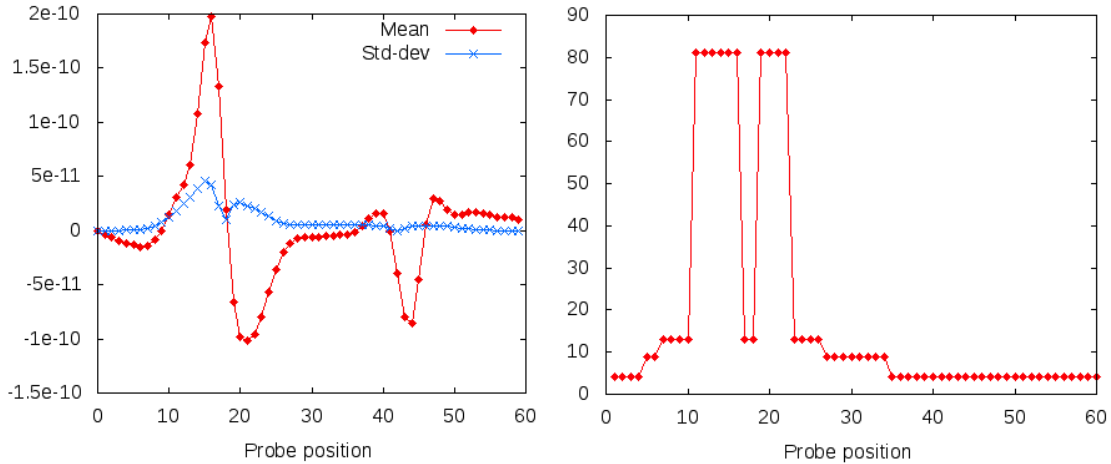
the relative permeability of TSP uniform on $[60, 100]$ and conductivity of TSP on the interval $[17E5, 18E5]$. From these prior distributions, we construct the PC response of the SAX ratio by the adaptive non-intrusive spectral projection described in section 3.2 and we compute the Sobol indices corresponding to the 4 random variables. In the inverse method, the experimental datum is taken from [11]. Applying the adaptive NISP, we obtain the probe random flux Φ as a (finite) third order PC expansion

$$\Phi(\xi) = \Phi(\xi_{\sigma}^m, \xi_{\mu_r}^m, \xi_{\sigma}^{\text{TSP}}, \xi_{\mu_r}^{\text{TSP}}) = \sum_{k=0}^{34} \Phi_k \Psi_k(\xi), \quad \Phi_k = \int_{[0,1]^4} \Phi(\xi) \Psi_k(\xi) d\xi,$$

in terms of the quadrivariate orthogonal Legendre polynomials Ψ_k , with uniformly distributed random variables as arguments. E.g., the magnetite's relative permeability is written as

$$\mu_r^m(\xi_{\mu_r}^m) = 1.3 + 1.4 \xi_{\mu_r}^m \quad \text{with} \quad \xi_{\mu_r}^m \sim U[0, 1].$$

The expansion coefficients Φ_k were computed with our adaptive sparse scheme. We calculate the Sobol index or sensitivity of the model to the input parameters.



(a) Mean and standard deviation of the imaginary part of the differential flux. (b) Number of deterministic simulations for each position of the probe.

Figure 3. Statistical moments and computational cost for each position of the probe.

In Fig. 3, we report the total number of deterministic simulations required by the adaptive NISP for each position of the probe. The lower edge of the support plate corresponds to the position 12 and the upper edge corresponds to the position 48. In Fig. 3(a), we see that the variability in the imaginary part of the flux is important in the upper part of the TSP and is negligible in lower part. Consequently, the number of deterministic simulations is higher (equal to 81) in upper edge and equal to 4 near the lower edge. This remark can be explained by the fact that uncertainties on the physical parameters of the TSP are insignificant and the flux is sensitive only on the uncertainties of the physical parameters of the magnetite. In fact, the variability of the flux is important only between position 10 and 22 of the probe which corresponds to the location of the magnetite.

The first order Sobol indices are computed using (3.3) and are represented in Fig. 3(c). We are interested in the sensitivity indices on the positions where the variability is important, i.e from position 12 to 22. In this region, the sensitivity of the relative permeability of the magnetite is up to 98%. Thus, the relative permeability of the magnetite is clearly

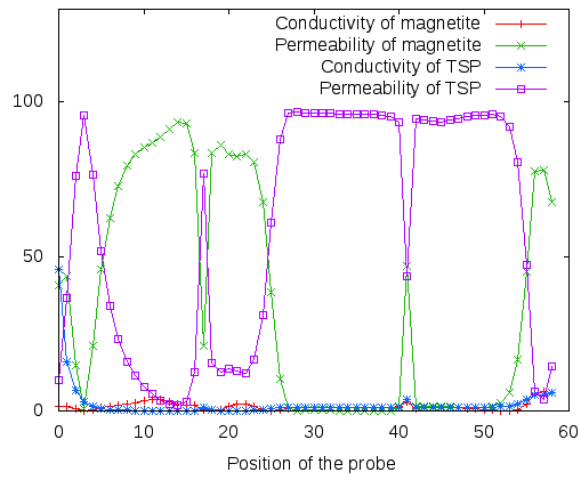
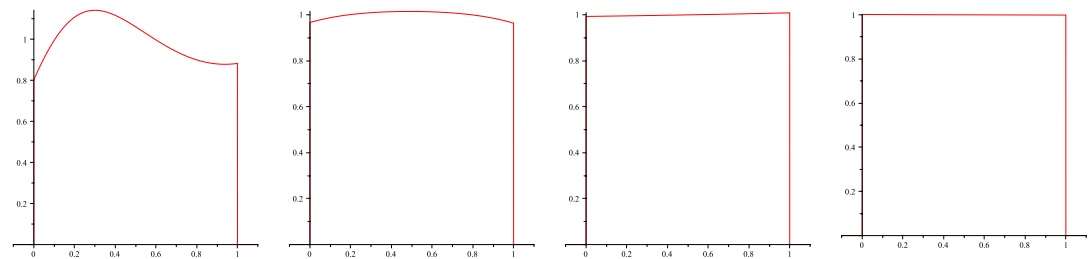


Figure 4. first order Sobol indices for each position of the probe.

the most influential random variable in the model. With the inverse method we will try to reduce its variability.

In the inversion procedure, the error is considered normally distributed with mean equal to 0 and a standard deviation $\sigma_\epsilon = 0.98$ obtained by the calibration technique described above. The marginal posterior densities of the four random variables are given in Fig. 5, again based on a sample of 25 SAX ratio measurements. Note that due to the PC expansion at hand the Bayesian procedure is cost effective. The density of the relative permeability of magnetite is clearly updated and reduced in variability.



(a) Relative permeability of the magnetite (b) Conductivity of the magnetite (c) Relative permeability of the TSP (d) Conductivity of the TSP

Figure 5. Marginal posterior densities of the random variables.

5. Conclusion

We dealt with the uncertainty quantification of the physical properties of magnetite (a corrosion product) which frequently clogs the tube support plate of a steam generator in a nuclear power plant. Using Polynomial Chaos (PC) in the direct approach combined with adaptive sparse grids, the prohibitive computational cost underlying the high dimensional random space in the direct Non-Intrusive Spectral Projection (NISP) method was mediated. This combination of techniques is most suitable for stochastic forward problems where not all stochastic dimensions are equally ‘important’ and thus can be discretized differently. This results in a more accurate model at the same computational cost, or one opts just to reduce computer time.

Some conditional posterior probability densities are identified by inferring from an experimental datum. We found agreement – with the Sobol indices and Bayesian inference – on the fact that the permeability of the magnetite is the most influential random variable in the model. Moreover the Bayesian technique reduced the variability in the permeability of the magnetite due to inference from experimental data. Inferring from more data can maybe further reduce the variability. The described technique enables to capture the probability density of a parameter that is hardly physically accessible. The efficiency of the method can possibly be improved by changing the PC expansion basis in the stochastic space. Furthermore the variance of the random flux can also be computed by the anisotropic adaptive NISP to improve/increase the polynomial interpolation/order based on the sparse grid.

References

- [1] BEDDEK, K., CLENET, S., MOREAU, O., COSTAN, V., LE MENACH, Y., AND BENABOU, A. Adaptive method for non-intrusive spectral projection – application on a stochastic eddy current NDT problem. *IEEE Transactions on Magnetics* 48, 2 (2012), 759–762.
- [2] BODINEAU, H., AND SOLLIER, T. Tube Support Plate Clogging Up of French PWR Steam Generators. In *Proceedings of EUROS SAFE Forum* (November 2008).
- [3] CHEN-CHARPENTIER, B., AND STANESCU, D. Parameter estimation using polynomial chaos and maximum likelihood. *International Journal of Computer Mathematics* 0, 0 (0), 1–11.
- [4] DE STAELEN, R. H., AND CREVECOEUR, G. A sensor sensitivity and correlation analysis through polynomial chaos in the EEG problem. *IMA Journal of Applied Mathematics* (2012).
- [5] DE STAELEN, R. H., CREVECOEUR, G., GOESSENS, T., AND SLODIČKA, M. Bayesian inference in the uncertain EEG problem including local information and a sensor correlation matrix. *Journal of Computational and Applied Mathematics* 252 (2013), 177–182.
- [6] GHANEM, R., AND SPANOS, P. D. *Stochastic Finite Element: A spectral approach*. Dover Publications, 2003.
- [7] HABER, E., AND HELDMANN, S. An octree multigrid method for quasi-static Maxwell’s equations with highly discontinuous coefficients. *Journal of Computational Physics* 223, 2 (2007), 783–796.
- [8] KAIPIO, J., AND SOMERSALO, E. *Statistical and Computational Inverse Problems*. Springer, 2005.
- [9] LIESE, F., AND MIESCKE, K.-J. *Statistical Decision Theory: Estimation, Testing, and Selection*. Springer, 2008.
- [10] MATEUS, L., STOLLENWERK, N., AND ZAMBRINI, J.-C. Stochastic models in population biology: from dynamic noise to bayesian description and model comparison for given data sets. *International Journal of Computer Mathematics* 0, 0 (0), 1–13.
- [11] MOREAU, O., COSTAN, V., DEVINCK, J.-M., AND IDA, N. Finite element modelling of support plate clogging in nuclear plant steam generators. In *Proceedings of NDE in Relation to Structural Integrity for Nuclear and Pressured Components* (2010).
- [12] SOBOL, I. Sensitivity estimates for nonlinear mathematical models. *Math. Modeling Comp. Exp.* 1 (1993), 407–414.
- [13] WIENER, N. The homogeneous chaos. *American Journal of Mathematics* 60, 4 (1938), 897–936.
- [14] XIU, D., AND KARNIADAKIS, G. The wiener-asky polynomial chaos for stochastic differential equations. *SIAM J.Sci. Comput.* 24, 2 (2002), 619–644.

List of changes